ISSN 2075-1087, Gyroscopy and Navigation, 2025, Vol. 16, No.1, pp. 94-102.

Algorithm for Determining the Depth of a Sound Source Using a Bottom Linear Antenna

A. I. Mashoshin*, V. S. Mel'kanovich, and V. N. Timofeev

Concern CSRI Elektropribor, JSC, St. Petersburg, Russia

**e-mail: aimashoshin@mail.ru*

Received: November 29, 2024; revised January 26, 2025; accepted April 1, 2025

Abstract: The paper describes an algorithm for determining the depth of a sound source using a multielement bottom linear antenna, based on measurements of differences in signal delays in a multipath channel. The accuracy of the algorithm is confirmed by simulation and verified experimentally.

Keywords: hydroacoustics, bottom linear antenna, determining the depth of a submerged sound source.

1. INTRODUCTION

Hydroacoustic surveillance systems are intended to detect marine intruders that cross the border of a protected area [1–3]. These systems are usually bottom low-frequency linear arrays (LFLA) consisting of acoustic receivers spaced at a distance from units to tens of meters from each other [1].

The main objective of such LFLA is to identify intruders (usually submarines, manned and unmanned underwater vehicles) from a variety of objects crossing the border. Normally, it is not problematic for LFLA to detect them. The situation is more complicated with their classification. The identification of an intruder as an underwater or surface object is commonly based the differences between the spectra of the carrier and amplitude envelopes of such objects [4–12]. However, the problem is that an underwater intruder can effectively adjust its noise profile to that of a surface ship, this being a well-proven technology. US Navy submarines, for instance, are equipped with systems that allow a submarine noise to be masked as a noise of a surface ship.

In view of the above, it is of practical interest to create alternative methods and algorithms for classification of underwater intruders. In this sense, the most effective method is to determine the depth of the detected object, since it is rather difficult to artificially disguise this parameter.

The distance and depth of a sound source can be calculated based on the multipath propagation of a source signal in an ocean waveguide [14]. The essence of this method lies in the fact that the autocorrelation function (ACF) of the source broadband noise shows the correlation maximums (CM) (Fig. 1) caused by coherent signals propagating along different acoustic rays. The abscissa of each CM is equal to the relative delay of the arrival of each pair of rays at the antenna, and the width, to the inverse value of the signal frequency band.

Since this delay carries information about the source coordinates, solving a system of equations that relate these coordinates to the value of the relative delay of acoustic rays, it is possible, in theory, to determine the source location.

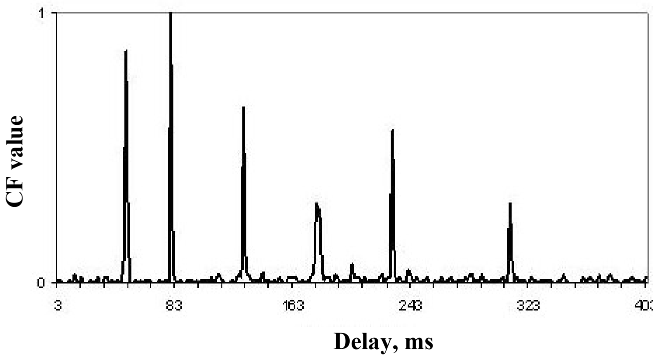

Fig. 1. An ACF of a sound source multipath broadband signal. The graph starts with a 3-ms delay to exclude the highest correlation maximum at zero delay that does not carry any useful information.

A large number of algorithms have been developed to implement this method in practice [13–23]. At the same time, the studies have shown that both the method itself and the algorithms implementing it have a significant drawback, which is the ambiguity of the result obtained. This drawback can be eliminated with the use of additional information.

This paper proposes an algorithm for determining the depth of a sound source, which allows classifying objects passing over a bottom linear antenna.

2. JUSTIFICATION OF THE ALGORITHM

The geometry of the problem is illustrated in Fig. 2.

Several acoustic rays, along which the object noise is propagated, arrive at the input of each LFLA receiver. We distinguish two of them:

- a direct ray (red line);
- a ray once reflected from the sea surface (green line).

They differ from the other rays in that they are most intense due to the minimum number of reflections from the waveguide boundaries, and therefore, the corresponding CM in the ACF has the highest level.

The relative delays in the arrivals of the two distinguished rays at the receiver is given as

$$\tau_{12} = \frac{\sqrt{R^2 + 4 \cdot H_m \cdot H_o} - R}{c}, \qquad (1)$$

where R is the slant (shortest) distance between the object and the receiver; H_m is the sea depth; H_o is the depth of the object-intruder; c is the average speed of the sound signal propagation in the waveguide calculated based on the measured vertical distribution of the sound velocity.

The magnitude of the relative delay τ_{12} is determined as follows: first, the ACF of the source broadband noise is calculated at the receiver output, where the object noise has the highest level (this receiver is designated as Receiver m_o), then, the CM with the largest value is identified in it, and, finally, its abscissa is found, which is equal to the sought delay τ_{12}.

Since the sea depth H_m in the area where the LFLA is installed and the parameters of τ_{12} and c are known, to calculate the depth H_o of the submerged object from formula (1), it is necessary to find the slant distance R between the source and Receiver m_o. For this purpose, we use the range-difference method [24], based on measuring delays of signal arrivals at three receivers, determined as the abscissas of the largest CMs in the cross-correlation function (CCF) of the signals at the output of each pair of the receivers.

Let us select 3 receivers: Receiver m_o, with the highest level of the object noise, and two more, Receivers m_{-1} and m_{+1}, symmetrically located relative to the first one. It is essential that the distance L between the receivers be maximum, but not exceed the signal coherence interval (30–40 wavelengths at frequencies below 1 kHz and 50 wavelengths at frequencies above 1 kHz) at the upper frequency of the frequency range used to measure the CCF [25]. It should be noted that the coherence interval values given are rather averaged and are valid for open water areas. In shallow areas with difficult relief of the seabed and configuration of the vertical distribution of sound velocity, the coherence interval can be significantly smaller.

In this manner, we determine the relative delay τ_- between the source signals at the outputs of Receivers m_o and m_{-1}, as well as the relative delay τ_+ at the outputs of Receivers m_o and m_{+1}, and then calculate the slant distance between the source and Receiver m_o by the formula:

$$R = \frac{2 \cdot L^2 - c^2 \cdot \left(\tau_+^2 + \tau_-^2\right)}{2 \cdot c \cdot \left(\tau_+ + \tau_-\right)}. \qquad (2)$$

Together with the slant distance, using the measured delays τ_- and τ_+, we can calculate angle α (Fig. A1) with the vertex at the point where Receiver m_o is located between the antenna line and the direction to the object:

$$\alpha = \arccos \frac{\left(c \cdot \hat{\tau}_- + R\right)^2 - \left(c \cdot \hat{\tau}_+ + R\right)^2}{4 \cdot L \cdot R}. \qquad (3)$$

Formulas (2) and (3) are derived in the appendix.

As a result, from Formula (1), we obtain the depth of the object's location:

$$H_o = \frac{\left(c \cdot \tau_{12} + R\right)^2 - R^2}{4 \cdot H_m}. \qquad (4)$$

The described algorithm is efficient when the following two conditions are met:

(1) the CM level in the ACF and CCF exceeds the specified threshold value under the background fluctuations;
(2) the RMS error of the CM abscissa measurements is significantly lower than the measurand.

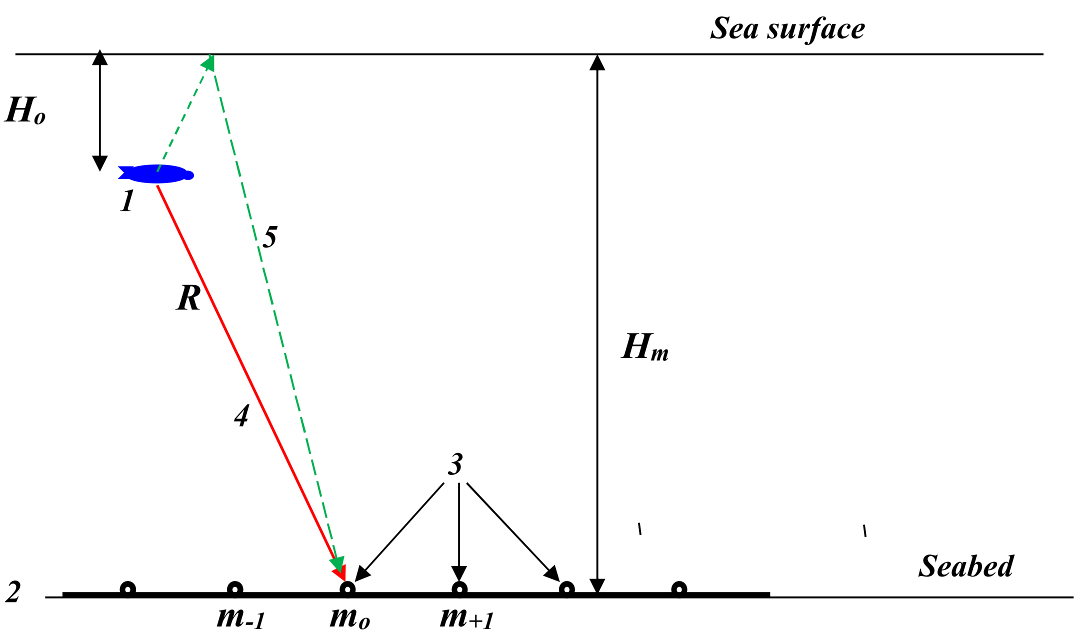

Fig. 2. Geometry of the problem: (1) intruder; (2) linear antenna of the LFLA; (3) LFLA receivers; (4) direct acoustic ray along which the intruder noise is propagated to the LFLA; (5) acoustic ray once reflected from the sea surface; H_m – sea depth; H_o – depth of the object-intruder; R – slant (shortest) distance between the object and Receiver m_o, at which the noise of the object has a maximum level.

The first condition is met if, under the assumption of complete coherence of the direct and reflected rays, the following inequality is valid [18, 19]:

$$Q_{ACF} = \sqrt{2 \cdot \Delta f \cdot T \cdot K_d \cdot K_{ref}} \cdot \frac{q}{(q+1)} > Q_{thr}, \quad (5)$$

where Q_{ACF} is the CM excess of the background fluctuations in the ACF, called output signal-to-noise ratio (SNR); Δf is the bandwidth in which ACF is calculated; T is the ACF accumulation time; K_d, K_{ref} is the ratio, respectively, of the power of the direct ray and the ray once reflected from surface to the total power of all rays at the receiver output; q is input SNR (in terms of power) in the frequency band Δf; Q_{thr} is the threshold value of the output SNR, usually equal to 5.

The second condition is satisfied if

$$\tau_{12} > 3 \cdot \sigma_\tau, \quad (6)$$

where σ_τ is the RMS error of the CM abscissa measurements in the ACF or CCF, defined as follows [26]:

$$\sigma_\tau = \frac{1}{\Delta f \cdot q}. \quad (7)$$

When the CCF is calculated under the assumption of coherence of the direct and reflected rays and in the absence of correlation of interference at the output of two spaced receivers, the first condition is satisfied if the following inequality is true [18, 19]:

$$Q_{CCF} = \sqrt{\frac{\Delta f \cdot T}{\left(1+q_1^{-1}\right) \cdot \left(1+q_2^{-1}\right)+1}} > Q_{thr}, \quad (8)$$

where q_i is the SNR at the output of the i-th receiver.

By periodically determining the slant distance and depth of the object, it is possible to calculate its motion parameters – heading K_o, speed V_o, and depth H_o.

3. ALGORITHM SIMULATION

The simulation was aimed to estimate the accuracy of determining the depth of an object, as well as the distance to it, based on a specific example.

The simulation was conducted for the following conditions:

- sea depth – 200 m;
- sound speed at the bottom – 1460 m/s;
- object depth – 180 m;
- distance between the receivers in the antenna – 20 m;
- the frequency band in which the CCF and ACF are calculated varies from 100 to 2000 Hz;
- the SNR (in terms of power) in the frequency band at the moment when an object is crossing the antenna line varies from –15 to +35 dB.

The horizontal projection of the object's path of motion relative to the antenna is shown in Fig. 3.

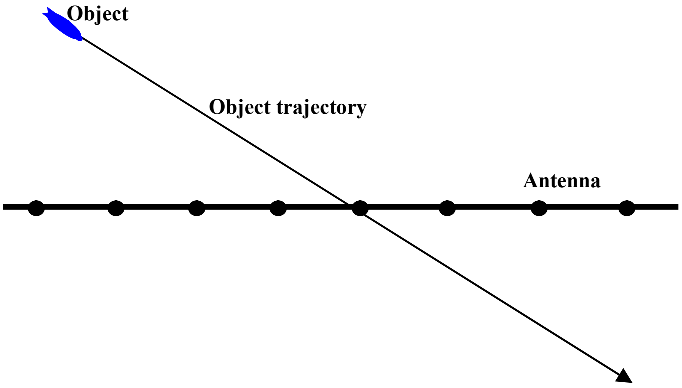

Fig. 3. Horizontal projection of the object's motion relative to the antenna.

The simulation consisted of the following:

- the frequency band and SNR values were selected from the specified intervals;
- the intervals of delay variations in the ACF and CCF were calculated for the depth of the object from 10 to 190 m. For the ACF, they were from 20 to 190 ms, and in the CCF – from 0 to 8.4 ms;
- the object's path of motion was calculated; in so doing, it was divided into intervals of measuring 10 accumulations of the ACF and CCF, each lasting 200 ms;
- for each *i*-th interval, the slant distance between the object and the nearest receiver was calculated, as well as the distance between the object and two neighboring receivers, those on the right and left;
- at the interval of each 200 ms-accumulation, digital methods were used to generate the object noise with a spectrum in the selected frequency band, decreasing according to the law of f^{-2};
- depending on the calculated distances, the generated noise of the object was recalculated at the outputs of the three receivers according to the spherical law;
- simultaneously, on the interval of each accumulation, a broadband interference was generated at the output of each of the three receivers, decreasing in accordance with the law of f^{-2};
- on each interval, the accumulated ACF signal-and-interference mixtures at the output of the receiver closest to the object and two CCF of the signal-and-interference mixtures at the output of the receiver closest to the object and each of the neighboring receivers were calculated. An example of the calculated ACF is shown in Fig. 4, and the CCF, in Fig. 5;

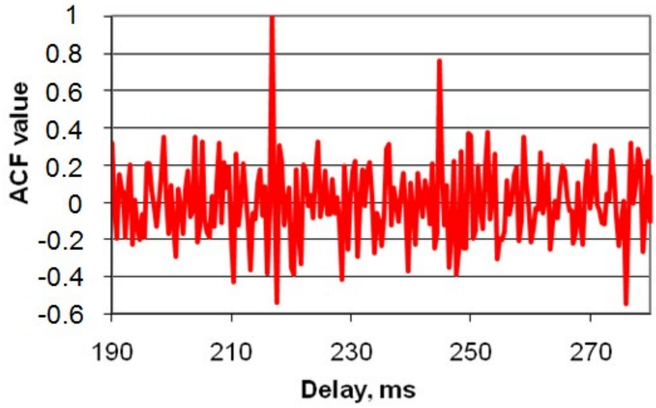

Fig. 4. An example of the calculated ACF with the highest CM for a delay of 216.8 ms caused by the interference of the direct ray and the ray once reflected from the surface, and the second highest CM for a delay of 244.8 ms caused by the interference of the direct ray and the ray once reflected from the seabed and then from the surface.

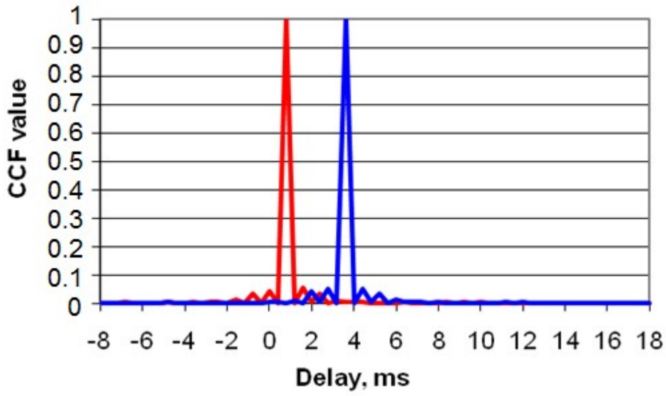

Fig. 5. The calculated CCF of signals at the output of the receiver closest to the object and the one adjacent to it on the left (red line), as well as at the output of the receiver closest to the object and the one adjacent to it on the right (blue line). The CMs in the CCF correspond to the delays in the propagation of the object's noise to the corresponding receivers.

- in the calculated ACF, we identified 2 or 3 maximums that were highest against the background and determined their abscissas, then we compared them with the abscissas of the maximums identified in the previous processing cycles. Thus, we found the abscissa τ_{12} of the maximum corresponding to the interference of the direct ray and the ray that was once reflected from the surface. This procedure is necessary because, for various reasons, this maximum does not always exceed the background to the greatest extent. To illustrate this statement, in Fig. 6 we show, depending on time, the delays between the direct ray and the ray reflected from the surface (dashed green line), as well as between the direct ray and the ray reflected first from the seabed, then from the surface (dashed blue line), and also, the abscissa of the maximum of the greatest level (solid red line);

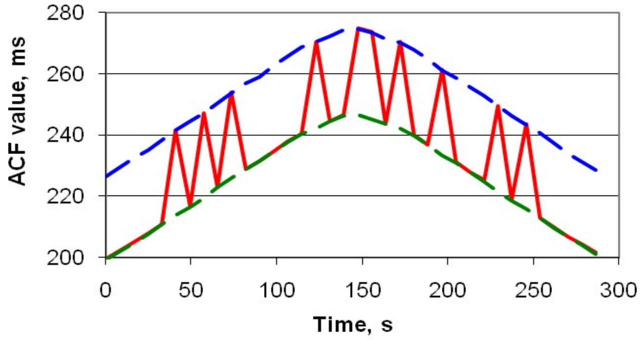

Fig. 6. The calculated delay-time dependences between the direct ray and the one reflected from the surface (dashed green line) and between the direct ray and the one reflected first from the seabed, then from the surface (dashed blue line), as well as the abscissa of the highest peak value in the simulated ACF (solid red line).

- in each of the two calculated CCFs, we identified narrowband CMs that significantly exceeded the background and determined their abscissas τ_- and τ_+. The dynamics of changes in the position on the axes of these abscissas and their theoretical values during the object motion are shown in Fig. 7;

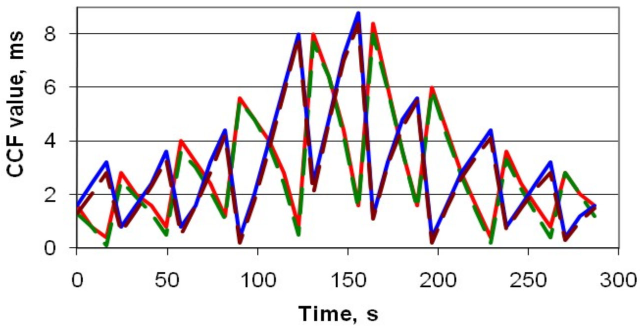

Fig. 7. Dynamics of the changes in the position on the abscissa axes of the largest CMs in the CCF (solid lines) and their theoretical values (dashed lines) during the object motion.

- formulas (2) and (4) were used to calculate the slant distance to the object R_i (the result is shown in Fig. 8) and the depth of the object H_i (the result is shown in Fig. 9);

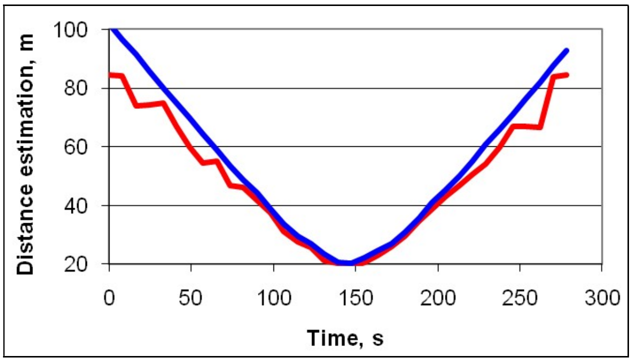

Fig. 8. Determination of the slant distance to an object while it was crossing the antenna line in a bandwidth of 1000 Hz for calculation of the CCF and the SNR 13.6 dB when the object was above the antenna. The blue line is the theoretical dependence, the red line is the simulation result.

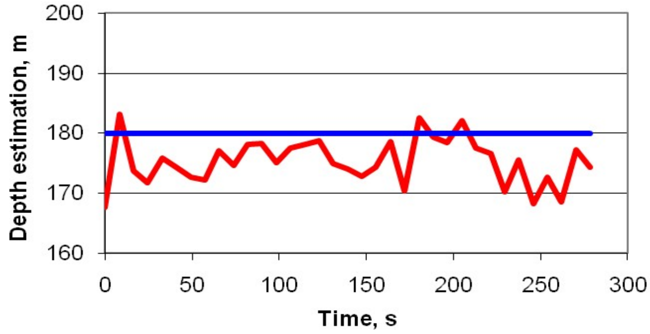

Fig. 9. Determination of the object’s depth while it was crossing the antenna line with a bandwidth of 1000 Hz for calculation of the CCF and the SNR 13.6 dB when the object was above the antenna. The blue line is the theoretical dependence, and the red line is the simulation result.

- the calculated values of these parameters were compared with their values specified based on the model of the object’s motion. The results obtained were used to calculate the estimation errors ΔR_i and ΔH_i;
- after the simulation of the object’s path, we calculated the RMS errors of the estimates of the slant distance and the object’s depth for the selected frequency band and SNR.

The simulation was performed for different combinations of the frequency band and SNR. The results are presented in Figs. 10 and 11.

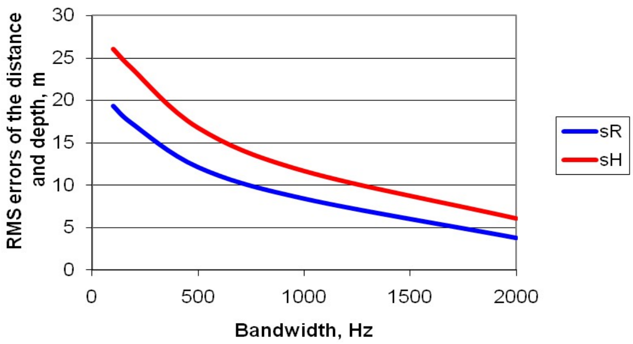

Fig. 10. Dependences of the RMS errors in the estimation of the distance to the object (blue line) and its depth (red line) in the bandwidth in which the ACF and CCF are calculated, with the SNR 13.6 dB at the moment when the object is passing over the antenna.

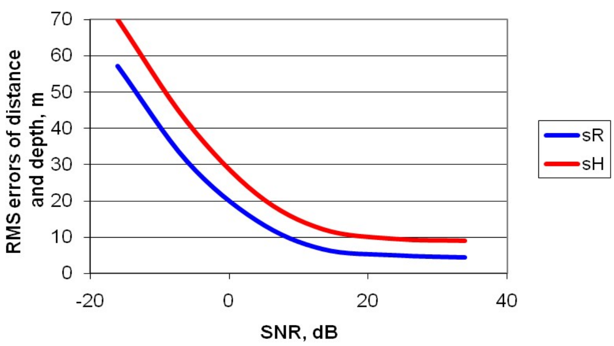

Fig. 11. Dependences of the RMS errors in the estimation of the distance to the object (blue line) and its depth (red line) on the SNR at the receiver output at the moment when the object is crossing the antenna line at a frequency band of 1000 Hz in which the ACF and CCF are calculated.

Figure 10 shows the dependences of the RMS errors of the distance and depth estimates on the frequency band, and Fig. 11, on the SNR.

It follows from the figures:

- with the SNR 13.6 dB at the moment of the object passing over the antenna and a frequency band greater than 1000 Hz, the RMS error in the estimation of the distance to the object does not exceed 8 m, and the object depth, 12 m;
- at a frequency band of 1000 Hz and the SNR 10 dB at the moment of the object passing over the antenna, the distance and depth are determined with similar accuracy.

In conclusion, we should make an important remark. The simulation results were obtained for the case when antenna has only one noisy object within its view. If there are more than one sound sources, the number of CMs in the ACF and CCF increases many times, which significantly complicates the problem solution, since the algorithm will be generating coordinates of not only real objects, but false ones as well. In addition, there may be a situation when the calculations of the distance and depth calculated by formulas (2) and (4) will use the CM in the ACF corresponding to one object, and the CM in the CCF, to another one.

The way out of this situation is to trace the distance and depth estimates in time, which will allow rejecting false objects.

4. EXPERIMENTAL VERIFICATION OF THE ALGORITHM

The algorithm was verified using the experimental data obtained during the tests of an engineering fiber-optic towed streamer in the waters of Lake Ladoga in 2022 [27]. A 100 m long towed streamer, consisting of 309 fiber-optic sensors, was laid on the seabed at a depth of 23 m. The sound speed all over the entire water layer was constant – 1430 m/s.

The distance from the towed streamer to the shore did not exceed 500 m. The coordinates of the towed streamer ends were determined with the receiver of a differential satellite navigation system (DSNS). During the tests, signals from each antenna receiver in the frequency band of up to 4 kHz were stored in the laptop memory with precise time reference.

A broadband acoustic generator, used as a noisy object, was towed by a boat at a speed of 1.0 m/s at a depth of 12.5 m. The boat coordinates were determined with the DSNS and stored in the laptop memory with precise time reference. The experimental data were processed using the methodology described above. The duration of one processing cycle was 0.5 s.

During data processing it became clear that there were a lot of local noise sources in the test area that showed themselves as a large number of CMs in the ACF and CCF formed by both direct signals from sources and their reflections from the seabed, surface and coastline. An example of the calculated ACF is shown in Fig. 12.

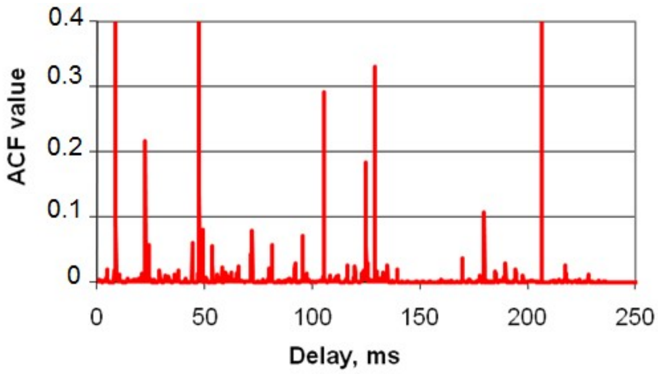

Fig. 12. An example of the ACF calculated with the use of experimental data. For the sake of clarity, the largest CM with zero delay that does not carry any useful information is excluded from the graph.

Therefore, the following measures were taken to identify the emitter's trajectory:

- the delay ranges in the ACF and CCF corresponding to the depth of the region and possible distances between the object and the towed streamer were calculated; during signal processing, the CMs were identified in the ACF and CCF only within these ranges;
- the coordinates of the objects calculated at each processing cycle were traced in time, which made it possible to reject stationary and false sources.

Figure 13 shows the results obtained during the experiment, when the emitter was moving away from the towed streamer at a speed of 1 m/s. The red line corresponds to the estimates of the slant distance to the object, the blue one, to the estimates of the depth of the object's location.

The dashed lines show the real values of the distance and depth. The average errors in the distance and depth estimates were 5.3 and 7.9 m, and the RMS fluctuation errors in determining the distance and depth were 7.7 m and 6.9 m, respectively.

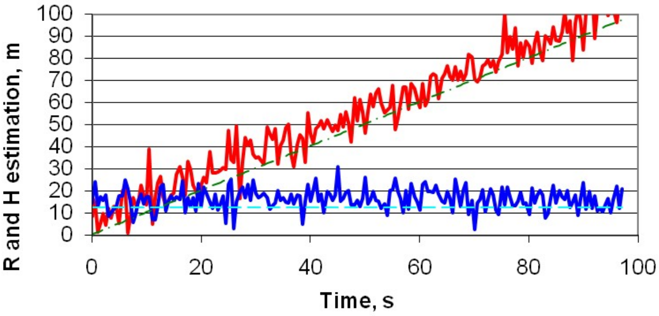

Fig. 13. Determination of the slant distance (red line) and depth (blue line) of an object when the emitter is moving away from the towed streamer line at a speed of 1 m/s. The dashed lines indicate the real distance and depth.

5. CONCLUSIONS

1. An algorithm has been developed which allows us, using a linear bottom hydroacoustic antenna, to determine the depth at which marine objects cross it, as well as other parameters of their motion, such as heading, speed, and current slant distance to the antenna.

2. The algorithm is based on the calculation of the delays between the signal rays along which the broadband noise of the object is propagated. The algorithm consists in the calculation of the autocorrelation function of the object's broadband noise at the output of the antenna receiver, corresponding to the maximum signal-to-noise ratio, and two cross-correlation functions of the signals at the output of this receiver and each of the two receivers on the left and right, located from the middle receiver at a distance close to (but not exceeding) the interval of spatial correlation of the signal at the upper frequency of the frequency range used.

3. The conditions for the feasibility of the proposed algorithm have been studied. It is shown that the main factors that influence the accuracy of determining the object's coordinates are the bandwidth used to calculate the correlation functions and the signal-to-noise ratio at the receiver output when the object is passing over the antenna.

4. The algorithm performance has been verified by simulation and experimentally.

APPENDIX

Derivation of Formulas for the Calculation of the Object Coordinates and Motion Parameters

Figure A1 shows a linear bottom equidistant hydroacoustic antenna. Consider a plane Cartesian coordinate system fixed to the seabed with the center at the location of Receiver m_o, the X-axis directed along the antenna line, and the Y-axis oriented perpendicular to the antenna line.

It is required to determine the slant distance R to the object from Receiver m_o, angle α with the vertex at the location of Receiver m_o between the antenna line and the direction to the object, the object speed V and the object heading γ relative to the receiver line.

The delays in the signal arrival of object O at Receivers m_o and m_{-1}, as well as at Receivers m_o and m_{+1}, are determined as

$$\hat{\tau}_- = \frac{\sqrt{R^2\cdot\sin^2\alpha + (L + R\cdot\cos\alpha)^2} - R}{c},\qquad \hat{\tau}_+ = \frac{\sqrt{R^2\cdot\sin^2\alpha + (L - R\cdot\cos\alpha)^2} - R}{c}, \tag{A1}$$

where $\hat{\tau}_-, \hat{\tau}_+$ are the delays of the object signal arrival at Receivers m_o and m_{-1} and Receivers m_o and m_{+1}, respectively; R is the sought distance between the object and Receiver m_o; α is the sought angle between the receiver line and the direction to the object; L is the distance between adjacent receivers; c is the speed of sound at the depth.

After squaring both parts of the both equations (A1) and carrying out simple transformations, we obtain:

$$(c\cdot\hat{\tau}_- + R)^2 = R^2 + L^2 + 2\cdot L\cdot R\cdot\cos\alpha,\qquad (c\cdot\hat{\tau}_+ + R)^2 = R^2 + L^2 - 2\cdot L\cdot R\cdot\cos\alpha. \tag{A2}$$

In (A2), the second equation is subtracted from the first one:

$$(c\cdot\hat{\tau}_- + R)^2 - (c\cdot\hat{\tau}_+ + R)^2 = 4\cdot L\cdot R\cdot\cos\alpha, \tag{A3}$$

from where

$$\cos\alpha = \frac{(c\cdot\hat{\tau}_- + R)^2 - (c\cdot\hat{\tau}_+ + R)^2}{4\cdot L\cdot R}. \tag{A4}$$

Substituting (A4) into the first equation (A2), we obtain

$$(c\hat{\tau}_- + R)^2 = R^2 + L^2 + 2LR\times \times\frac{(c\cdot\hat{\tau}_- + R)^2 - (c\cdot\hat{\tau}_+ + R)^2}{4LR}. \tag{A5}$$

After simple transformations we derive

$$(c\cdot\hat{\tau}_-)^2 + 2c\cdot\hat{\tau}_-\cdot R + (c\cdot\hat{\tau}_+)^2 + 2c\cdot\hat{\tau}_+\cdot R = 2L^2, \tag{A6}$$

from where

$$R = \frac{2\cdot L^2 - c^2\cdot(\hat{\tau}_-^2 + \hat{\tau}_+^2)}{2\cdot c\cdot(\hat{\tau}_- + \hat{\tau}_+)}. \tag{A7}$$

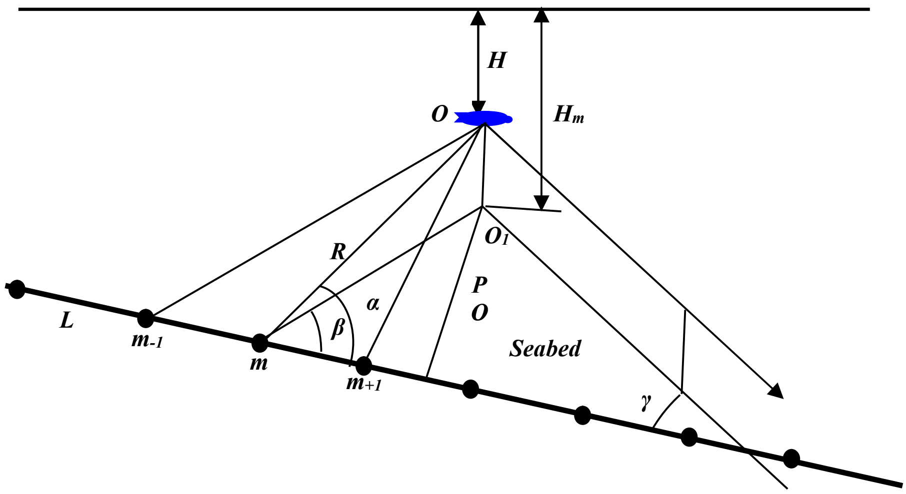

Fig. A1. Illustration of determining the coordinates and parameters of an object's motion

As a result, the distance to the object is calculated by formula (A7); the cosine of the angle between the receiver line and the direction to the object, by formula (A4).

The Cartesian coordinates of the object at moment t_1 of measuring the slant distance to the object are written as

$$Y_1 = R \cdot \cos\alpha,$$
$$X_1 = \sqrt{R^2 - (H_s - H_o)^2 - R^2 \cdot \cos^2\alpha} = \sqrt{R^2(1 - \cos^2\alpha) - (H_s - H_o)^2}, \quad \text{(A8)}$$

where H_s is the sea depth at the antenna location.

When redetermining the slant distance R and angle α relative to a certain receiver m_2 at time t_2 and using them to calculate the object coordinates X_2, Y_2, the object's speed V and heading γ relative to the receiver line can be calculated by the formulas:

$$V = \frac{\sqrt{(X_2 - X_1)^2 + (Y_2 - Y_1)^2}}{t_2 - t_1}, \quad \gamma = \mathrm{arctg}\frac{Y_2 - Y_1}{X_2 - X_1}. \quad \text{(A9)}$$

FUNDING

This work was supported by ongoing institutional funding. No additional grants to carry out or direct this particular research were obtained.

CONFLICT OF INTEREST

The authors of this work declare that they have no conflicts of interest.

REFERENCES

1. *GAK MGK-608E*. Official website of AO NII Atoll. https://www.niiatoll.ru. Accessed December 02, 2025.
2. *SOSUS* (Sound surveillance system). https://ru.wikipedia.org. Accessed December 02, 2025.
3. *IUSS* (Integrated undersea surveillance system). https://ru.wikipedia.org. Accessed December 02, 2025.
4. Telyatnikov, V.I., Methods and devices for classification of hydroacoustic signals, *Zarubezhnaya radioelektronika*, 1979, no. 9, pp. 19–38.
5. Koryakin, Yu.A., Smirnov, S.A., and Yakovlev, G.V., *Korabel'naya gidrolokatsionnaya tekhnologiya. Sostoyanie i tekushchye problemy* (Shipborne Sonar Technology. Status and Current Problems), St. Petersburg: Nauka, 2004.
6. *Spravochnik po gidroakustike* (Handbook of Hydroacoustics). Leningrad: Sudostroyeniye, 1988.
7. Lourence, J.G., Classification of ships using underwater radiated noise, Underwater Acoustic Data Processing,Y.T. Chan, Ed., *Proceedings of NATO Advanced Study Institute*, 1989, pp. 591–596.
8. Mashoshin, A.I., Features of the synthesis of algorithms for the classification of marine objects by their hydroacoustic field, *Morskaya radioelektronika*, 2009, no. 2 (28), pp. 8–12.
9. Marasev, S.V., Mashoshin, A.I., and Podshivalov, G.A, Russian Federation Patent no. 2681526, *Method for Determining the Class of a Noisy Target and the Distance to It*. Claimed 22.02.2018, published 07.03.2019, Byulleten' no. 2.
10. Marasev, S.V., Mashoshin, A.I., and Podshivalov, G.A, Russian Federation Patent no. 2746581, *Method for determining the class of a noisy marine object*. Claimed 26.05.2020, published 19.04.21, Byulleten' no. 11.
11. Marasev, S.V., Mashoshin, A.I., and Podshivalov, G.A, Russian Federation Patent no. 2681432. *Method for determining the class of a noisy marine object and distance to It*. Claimed 12.04.2018, published 06.03.2019, Byulleten' no. 2.
12. Marasev, S.V., Mashoshin, A.I., and Podshivalov, G.A, Russian Federation Patent no. 2685419, *Method for*

Determining the Class of a Noisy Target, Claimed 04.05.2018, published 18.04.2019, Byulleten' no. 11.

13. Quazi, A.H. and Lerro, D.T., Passive localization using time-delay estimates with sensor positional errors, *JASA*, 1985, vol. 78, no. 5, pp. 1664–1670. https://doi.org/10.1121/1.392805
14. Hassab, I.C., Contact Localization and Motion Analysis in the Ocean Environment: a Perspective, *IEEE Journal of Oceanic Engineering*, 1983, vol. OE-8, no. 3, pp.136–147.
15. Worthmann, B.M., Song H.C., and Dowling, D.R., High frequency source localization in a shallow ocean sound channel using frequency difference matched field processing, *Journal Acoust. Soc. Am.*, 2015, vol. 138, p. 35–49. https://doi.org/10.1121/1.4936856
16. Orlov, E.F., Fokin, V.N., and Sharonov G.A., Study of wideband sound interference modulation parameters in a deep ocean, *Acoustic Journal*, 1988, no. 34, p. 902–907.
17. Lazarev, V.A., Orlov, E.F., Fokin, V.N., and Sharonov, G.A., Frequency dependence of interference modulation parameters wideband sound in a shallow sea, *Acoustic Journal*, 1989, no. 35, p. 685–688.
18. Mashoshin, A.I., Multipath maximums in the correlation function of a wideband noise signal produced by a sea object: noise immunity of their extraction, *Acoustic Journal*, 2001, no. 47, p. 823–829.
19. Mashoshin, A.I., Study of the applicability conditions of the correlation function of a wideband multipath signal for estimating source coordinates, *Acoustic Journal*, 2017, no. 63, p. 307–313. https://doi.org/10.7868/S0320791917030091
20. Mashoshin, A.I., and Mel'kanovich, G.A, Russian Federation Patent no. 2690223. *Method for Determining a Marine Noisy Target*. Claimed 28.08.2018, published 31.05.2019, Byulleten' no. 16.
21. Grinenkov, A.V., Mashoshin, A.I., and Mel'kanovich, G.A, Russian Federation Patent no. 2724962. *Method for Determining Coordinates of a Marine Noisy Target*. Claimed 27.11.19, published 29.06.2020, Byulleten' no. 19.
22. Grinenkov, A.V., Mashoshin, A.I., and Mel'kanovich, G.A, Russian Federation Patent no. 2797161. *Method for Determining Coordinates of a Marine Noisy Target*. Claimed 27.09.22, published 31.05.23, Byulleten' no. 16.
23. Grinenkov, A.V. and Mashoshin, A.I., Russian Federation Patent no. 2812119. *Method for Determining Coordinates of a Marine Noisy Target*. Claimed 27.09.22, published 23.01.24, Byulleten' no. 3.
24. Telyatnikov, V.I., Methods and devices for determining the location of the sound source, *Zarubezhnaya radioelektronika*, 1978, no. 4, pp. 66–86.
25. Carey, W.M., The determination of signal coherence length based on signal coherence and gain measurements in deep and shallow water, *J. Acoust. Soc. Am.*, 1998, vol. 104, pp. 831−837.
26. Kozick, R.J., Sadler, B.M., Communication channel estimation and waveform design: time delay estimation on parallel, flat fading channel, *US Army research laboratory*, 2010, 42 p.
27. *Kontsern "TSNII "Elektropribor" vpervye predstavil proekt sozdaniya morskikh seismorazvedochnykh buksiruemykh kos* (Concern CSRI Elektropribor presented for the first time a project for the creation of marine towed streamers). https://news/comments/koncern_cnii_elektropribor_vpervye_predstavil_proekt_po_sozdaniyu_morskih_seysmicheskih_buksiruemyh_kos.html